Talanta 234 (2021) 122620

Contents lists available at ScienceDirect

Talanta

journal homepage: www.elsevier.com/locate/talanta

Rapid quantification of extracellular neurotransmitters in mouse brain by PESI/MS/MS and longitudinal data analysis using the R and Stan-based Bayesian state-space model

Daisuke Kawakami [a,b], Mitsuki Tsuchiya [a], Tasuku Murata [b], Akira Iguchi [c], Kei Zaitsu [a,d,*]

[a] Department of Legal Medicine & Bioethics, Nagoya University Graduate School of Medicine, 65 Tsurumai-cho, Showa-ku, Nagoya, 466-8550, Japan
[b] Shimadzu Corporation, 1, Nishinokyo-Kuwabaracho Nakagyo-ku, Kyoto, 604-8511, Japan
[c] Geological Survey of Japan, National Institute of Advanced Industrial Science and Technology (AIST), Tsukuba, Ibaraki, 305-8567, Japan
[d] In Vivo Real-time Omics Laboratory, Institute for Advanced Research, Nagoya University, Furo-cho, Chikusa-ku, Nagoya, 464-8601, Japan

ARTICLE INFO

Keywords:
Probe electrospray ionization/tandem mass spectrometry
Microdialysis
Quantitative analysis
Neurotransmitter
High-k+ induced depolarization
R and stan-based bayesian state-space model

ABSTRACT

We developed a methodology for rapid quantification of extracellular neurotransmitters in mouse brain by PESI/MS/MS and longitudinal data analysis using the R and Stan-based Bayesian state-space model. We performed a rapid analysis for quantifying extracellular L-glutamic acid (L-Glu) and gamma-aminobutyric acid (GABA) in the mouse striatum by combined use of probe electrospray ionization/tandem mass spectrometry (PESI/MS/MS) and in vivo brain microdialysis. We optimized the PESI/MS/MS parameters with the authentic L-Glu, GABA, L-Glu-$^{13}C_5$,$^{15}N_1$, and GABA-D_6 standards. We constructed calibration curves of L-Glu and GABA with the stable isotope internal standard correction method (L-Glu-$^{13}C_5$,$^{15}N_1$, and GABA-D_6), demonstrating sufficient linearity ($R > 0.999$). Additionally, the quantitative method for L-Glu and GABA was validated with low-, middle-, and high-quality control samples. The intra- and inter-day accuracy and precision were 0.4%–7.5% and 1.7%–5.4% for L-Glu, respectively, and 0.1%–4.8% and 2.1%–5.7% for GABA, respectively, demonstrating high reproducibility of the method. To evaluate the feasibility of this method, microdialyses were performed on free-moving mice that were stimulated by high-K^+-induced depolarization under different sampling conditions: 1) every 5 min for 150 min ($n = 2$) and 2) every 1 min for 30 min ($n = 3$). We applied the R and Stan-based Bayesian state-space model to each mouse's time-series data considering autocorrelation, and the model successfully detected abnormal changes in the L-Glu and GABA levels in each mouse. Thus, the L-Glu and GABA levels in all microdialysates approximately increased up to two- and seven-fold levels through high-K^+-induced depolarization. Additionally, a 1-min temporal resolution was achieved using this method, thereby successfully monitoring microenvironmental changes in the extracellular L-Glu and GABA of the mouse striatum. In conclusion, this methodology using PESI/MS/MS and Bayesian state-space model allowed easy monitoring of neurotransmitters at high temporal resolutions and appropriate data interpretation considering autocorrelation of time-series data, which will reveal hidden pathological mechanisms of brain diseases, such as Parkinson's disease and Huntington's disease in the future.

1. Introduction

Neurotransmitters play an important role in neural communications in the brain. Moreover, L-glutamic acid (L-Glu) and gamma-aminobutyric acid (GABA) are mainly involved in the excitatory and inhibitory neural communications, respectively. The basal ganglia circuits are essential for adaptive motor control and procedural memory [1]. The striatum, which comprises the basal ganglia circuits, receives excitatory inputs that are mediated by L-Glu from the cerebral cortex and thalamus. The striatum is rich in GABA-mediated inhibitory neurons; medium spiny neurons, which project to the globus pallidus internus (GPi); and the substantia nigra pars reticulata (SNr) as the direct pathway, and indirectly connects to GPi/SNr via the globus pallidus externus (GPe) and subthalamic nucleus (STN) [2–4]. The

* Corresponding author. In Vivo Real-time Omics Laboratory, Institute for Advanced Research, Nagoya University, Furo-cho, Chikusa-ku, Nagoya, 464-8601, Japan.
E-mail address: kzaitsu@med.nagoya-u.ac.jp (K. Zaitsu).

https://doi.org/10.1016/j.talanta.2021.122620
Received 28 April 2021; Received in revised form 11 June 2021; Accepted 12 June 2021
Available online 17 June 2021

GABAergic and glutamatergic neuron dysfunctions are associated with representative neurological disorders, including Parkinson's disease (PD) and Huntington's disease (HD) [1,3,5,6]. Thus, it is essential to elucidate the behaviors of L-Glu and GABA in the brain to understand the neural activity, and there are many studies to monitor the neurotransmitters [7–9]; the reliable quantitative method for extracellular L-Glu and GABA using microdialysis have been strongly required.

Microdialysis is an established technique for collecting neurotransmitters and endogenous metabolites in an extracellular region, and it can be applied to living animals [10]. In microdialysis, a semipermeable membrane is mounted in a microdialysis probe, and the probe is implanted in the brain, enabling monitoring of the extracellular levels of neurotransmitters in a conscious free-moving animal. To quantitate the neurotransmitters in the microdialysates, which generally contain high concentration salts, the following analytical techniques were reported: liquid chromatography with fluorescence resonance energy transfer detection (LC–FL) [11], LC/laser-induced fluorescence (LC/LIF) [12], LC/electrochemical (LC/EC) detection [13], LC-triple quadrupole tandem mass spectrometry (LC/MS/MS) [7,8,14], and gas chromatography-tandem mass spectrometry (GC/MS/MS) [15]. Among them, LC/MS/MS has been recently used to analyze microdialysates because of its high selectivity. Furthermore, some researchers have used LC/MS/MS to determine the extracellular levels of L-Glu and GABA in different brain regions [7,16,17], although sample pretreatment is mandatory for LC/MS/MS and requires prolonged analysis time. Additionally, the quantitative results fluctuate depending on an operator's skill even when the internal standard (IS) correction methods are appropriately performed. Preferably, to eliminate the tedious sample preparation to avoid a bias from the final results, ambient ionization mass spectrometry (AI-MS) is applicable.

AI-MS has been recently applied to various scientific fields [18–21], and our group has reported that PESI/MS/MS could be applied to the direct analysis of compounds in various biological specimens [22–26]. PESI/MS/MS enables us to execute the direct analysis of targeted compounds without the time-consuming pretreatment. Moreover, it reduces the volume of the sample in spite of high concertation salts in microdialysates, improving the temporal resolution of the microdialysis technique.

Evidently, time-series data of neurotransmitters and metabolites are obtained from the microdialysis technique, and thus, appropriate longitudinal data analysis is essential for interpreting the data. In previous studies, statistical analyzes, such as analysis of variance parametric or non-parametric statistical test were performed for each time point data, which were obtained by averaging different individuals' values at each time point [8,27,28]. However, this approach is somewhat inappropriate for evaluating time-series data, which show autocorrelation for each individual. Thus, this method is unacceptable for time-series data because it leads to ignoring of the autocorrelation of the data. Ngernsutivorakul et al. proposed a new approach using a general linear model for detecting unusual changes beyond the basal values [29]. Alternatively, it is also acceptable to use a Bayesian state-space model for such time-series data, though no report has applied the Bayesian state-space model to time-series data obtained by microdialysis.

In this study, therefore, we reported a methodology for rapid quantification of extracellular L-Glu and GABA, which are representative excitatory and inhibitory neurotransmitters, in the mouse brain by PESI/MS/MS and longitudinal data analysis using the R and Stan-based Bayesian state-space model. Here we combined the use of PESI/MS/MS with a microdialysis technique for quantitating extracellular L-Glu and GABA in mouse striatum and constructed calibration curves of L-Glu and GABA in the artificial cerebrospinal fluid (aCSF), where the intra- and inter-day accuracy and precision were fully validated. Finally, we monitored the high-K^+-induced depolarization in the brain of a mouse, and successfully captured the extracellular profiles of L-Glu and GABA by the methodology using the R and Stan-based Bayesian state-space model.

2. Material and methods

2.1. Chemicals and reagents

LC/MS-grade formic acid (FA) and ethanol were purchased from FUJIFILM Wako Pure Chemical Corporation (Osaka, Japan). Sodium chloride (NaCl), potassium chloride (KCl), magnesium sulfate ($MgSO_4$), calcium chloride ($CaCl_2$), sodium dihydrogen phosphate (NaH_2PO_4), and disodium hydrogen phosphate (Na_2HPO_4) were purchased from FUJIFILM Wako Pure Chemical Corporation (Osaka, Japan). L-Glu (purity ≧99%) was purchased from Sigma (Tokyo, Japan), and GABA (purity > 98%) was purchased from Tokyo Chemical Industry Co., Ltd. (Tokyo, Japan). The stable L-Glu ($^{13}C_5$, $^{15}N_1$) (purity: ^{13}C, 98% and ^{15}N, 95%) isotope was purchased from Taiyo Nippon Sanso Corporation (Tokyo, Japan), and GABA (D_6) (purity: 98.8%) was purchased from Toronto Research Chemicals (Canada). These stable isotope-labeled compounds were employed as ISs, and their concentrations were 2000 and 20 ng mL^{-1} for L-Glu ($^{13}C_5$, $^{15}N_1$) and GABA (D_6), respectively. The IS solution was prepared by mixing ISs and 5% FA in 50% EtOH solution. The aCSF solution (pH 7.4) contained 145 mM NaCl, 2.68 mM KCl, 1.10 mM $MgSO_4$, 1.22 mM $CaCl_2$, 0.50 mM NaH_2PO_4, and 1.55 mM Na_2HPO_4. The high-K^+–aCSF solution (pH 7.4) contained 47.7 mM NaCl, 100 mM KCl, 1.10 mM $MgSO_4$, 1.22 mM $CaCl_2$, 0.50 mM NaH_2PO_4, and 1.55 mM Na_2HPO_4 [29].

2.2. Preparation of the calibrants and quality control samples

The stock standard solutions of L-Glu and GABA were prepared by solving the authentic standards of L-Glu and GABA with aCSF at 1 mg mL^{-1}. The calibrants for L-Glu were prepared by diluting the stock standard solution of L-Glu with 250, 1000, 2000, 5000, and 10000 ng mL^{-1} aCSF. The calibrants for GABA were prepared by diluting the stock standard solution of GABA with 2.5, 10, 20, 50, and 100 ng mL^{-1} aCSF. Quality control (QC) samples for L-Glu were prepared by diluting the stock standard solution of L-Glu with 800, 4000, and 8000 ng mL^{-1} aCSF. QC samples for GABA were prepared by diluting the stock standard solution of GABA with 8.0, 40, and 80 ng mL^{-1} aCSF. These standards were stocked at 4°C until the analysis.

2.3. Analytical conditions of PESI/MS/MS

A tandem mass spectrometer (LCMS-8040, Shimadzu, Kyoto, Japan) with a PESI ion source (Shimadzu, Kyoto, Japan) was used (Fig. 1). The parameters of the mass spectrometer were as follows: desolvation line temperature, 300°C; heat block temperature, 30°C; detection mode, selected reaction monitoring (SRM); mass resolution, unit mass; dwell and pause times; 10 and 1 ms, respectively. The polarity, SRM transitions, and collision energies of each compound are shown in Table 1. All targeted analytes were preinstalled in a method, and the data acquisition time was 0.5 min. The applied voltage of the probe was +2.5 kV, whereas the probe stroke speed and acceleration were 300 mm s^{-1} and 1.00 G, respectively.

2.4. Surgical procedures for microdialysis

The animal experiments were approved by the Animal Experiment Committee of Nagoya University Graduate School of Medicine (No. 31327). This procedure followed that of Fuwa et al. [30] with minor modifications. A male Institute of Cancer Research (ICR) mouse (10–13 weeks) was anesthetized by isoflurane and fixed to a stereotaxic frame (SR-5M-HT, Narishige, Tokyo, Japan). After removing the hair, the skull of the mouse was exposed and carefully drilled. A microdialysis probe (D-I-6-02, Eicom, Kyoto, Japan) was implanted in the striatum (anteroposterior, −0.7 mm; lateral, 2.2 mm from the bregma and 3.4 mm from the surface). The probe was fixed using a dental acrylic resin (Toughron rebase, Miki Chemical Product Co. Ltd., Kyoto, Japan). The

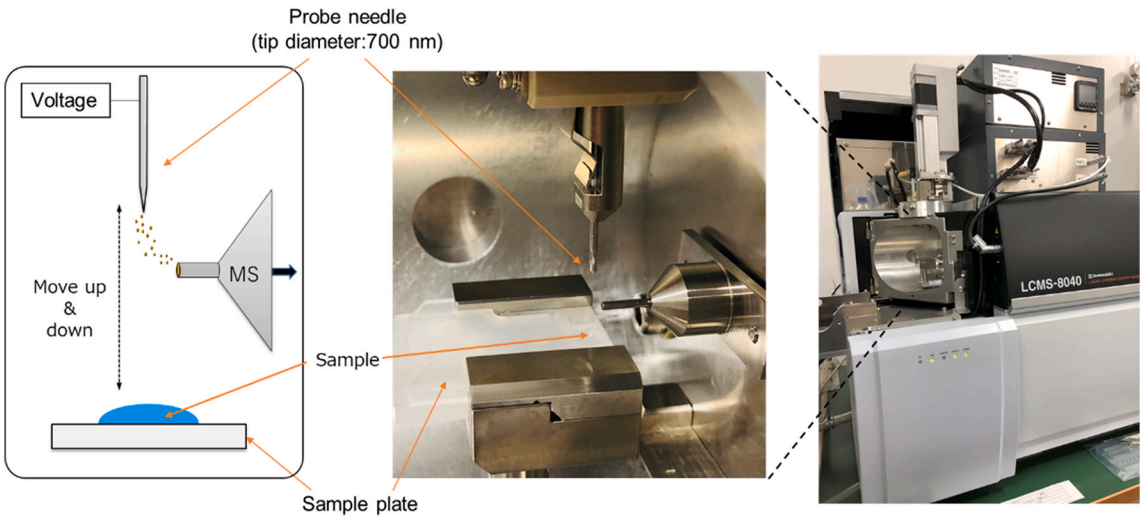

Fig. 1. Schematics of the probe ESI source combined with MS/MS.

Table 1
Polarity, SRM transitions, and collision energies that were used for PESI/MS/MS.

Compound name	Polarity	SRM transition	Collision energy (V)
L-glutamic acid	pos	*m/z* 148 > 84	15
L-glutamic acid-$^{13}C_5$,$^{15}N_1$	pos	*m/z* 154 > 89	15
GABA	pos	*m/z* 104 > 87	15
GABA-D_6	pos	*m/z* 110 > 93	15

pos: PESI positive mode.

mouse was allowed to recover overnight, and the microdialysis was performed the following day.

2.5. In vivo microdialysis procedure

aCSF was perfused at 3 μL min^{-1} with a syringe pump (KDS100, KD Scientific) and equilibrated for 2 h. We performed two experiments as follows:

1) Experiment 1: as shown in Fig. 2a, aCSF was perfused for 30 min after the equilibration. To facilitate the release of the neurotransmitter, aCSF was changed to high-K^+ aCSF for 60 min. Furthermore, aCSF was reperfused for 60 min after high-K^+ aCSF perfusion. The dialysates were collected at intervals of 5 min for 150 min (n = 2). 2) Experiment 2: as shown in Fig. 2b, aCSF was perfused for 10 min after the equilibration. To facilitate the release of the neurotransmitter, aCSF was changed to high-K^+ aCSF for 20 min. The dialysates were collected at intervals of 1 min for 30 min (n = 3).

2.6. Quantitative analysis of the microdialysates by PESI/MS/MS

To quantitate the microdialysate samples, we mixed 3 μL of each microdialysate sample with 12 μL of the IS solution, and the mixture was pipetted into a dedicated sample plate (Fig. 2c).

All peak areas in each chronogram were automatically integrated by the LabSolutions software (Shimadzu Corporation, version 5.86 SP1). The software parameters for automatic peak picking were as follows: drift (D), 0 min^{-1}; T. DBL (T), 1000 min; calculated data, area; width (W), 5 s; Slope (S), 1000 min^{-1}. All calculated peak areas (ACPA) were copied and pasted on an Excel (Microsoft, Excel 2016) worksheet. The IS correction was performed according to the following equation:

1) IS correction for L-Glu: (ACPA of L-Glu)/(ACPA of L-Glu-$^{13}C_5$, $^{15}N_1$)
2) IS correction for GABA: (ACPA of GABA)/(ACPA of GABA-D_6)

2.7. Bayesian state-space model

R and Stan [31] were employed to perform the Bayesian state-space model [32] to predict L-Glu and GABA basal levels in the microdialysate in each mouse with a 95% credible interval (CI). The following state equation was used [33] with minor modification. We ran 4 chains of 8000 from the posterior distribution and discarded the first 2000 ones before inference. Model diagnostics were confirmed by Rhat values.

$$\mu_{pred}(t+i) = \mathrm{Nomal}\left[2^{*}\mu_{pred}(t+i-1) - \mu_{pred}(t+i-2), \sigma\right] \quad \text{(Eq.1)}$$

Here, μ_{pred} (t) is level component and σ is standard deviation of process error.

We calculated 95% CI by substituting the first ten-point data of each mouse for this equation and determined that L-Glu and GABA levels changed significantly outside 95% CI. The 95% CI was shown in the color band for each figure.

3. Results and discussion

3.1. Optimization of the MS conditions and FA concentration

We optimized the MS parameters with authentic standards of L-Glu, GABA, L-Glu-$^{13}C_5$,$^{15}N_1$, and GABA-D_6. The optimal parameters are shown in Table 1. To enhance the ionization efficiency, PESI requires the supply of an organic solvent onto the tip of a probe needle [22,34]. In our previous studies, we used ethanol as an ionization enhancer and set its final concentration to 50% [22–26]. Thus, we diluted the microdialysate (3 μL) with a 50% ethanol aqueous solution (12 μL) and analyzed it, resulting in unsatisfactory reproducibility (Fig. S1). The peak areas of L-Glu and GABA fluctuated strongly (33% for both), indicating the instability of their ionization. Since the acid dissociation constants of L-Glu and GABA are 2.1 and 4.0, respectively, the ionization efficiencies were expected to be stable under acidic conditions. To stabilize their ionization efficiencies, FA was used to adjust the pH of the microdialysate to make it acidic. As shown in Fig. S1, we compared the 0.5 and 5.0% FA concentrations. The peak area value of L-Glu in the 5.0% FA solution (Ave. = 104129.2) was higher than that in the 0.5% FA solution (Ave. = 91785.1). Although the peak area values of GABA in the 0.5 and 5.0% FA solutions (Ave. = 12595.6 and 12023.6, respectively) were lower than those in the FA-free solutions (Ave. = 41258.8), the relative standard deviation (RSD) values of the GABA peak areas in the 0.5 and 5.0% FA solutions were dramatically improved (4.0% each). Consequently, the determined optimal concentration of FA was 5.0%.

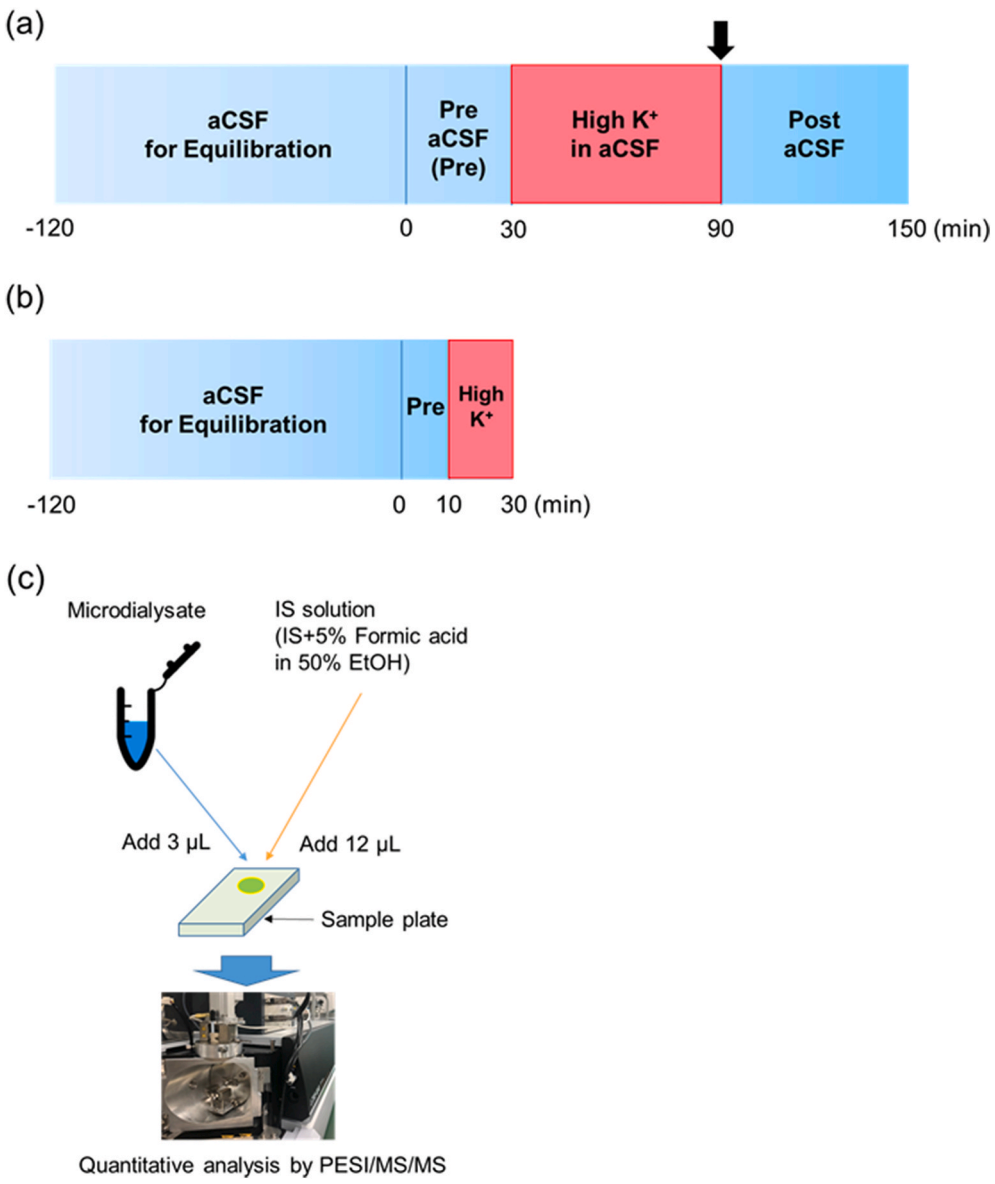

Fig. 2. In vivo microdialysis procedure. (a) Perfusion of aCSF started at 0 min, and 100 mM K^+ was perfused in aCSF for 30–90 min (red zone). Afterward, basal aCSF was reperfused (black arrows). Microdialysates were collected at 5-min intervals. (b) aCSF perfusion started at 0 min, and 100 mM K^+ was perfused in aCSF for 10–30 min (red zone). Microdialysates were collected at 1-min intervals. (c) Schematics of the measurement procedure by PESI/MS/MS. (For interpretation of the references to color in this figure legend, the reader is referred to the Web version of this article.)

3.2. Method validation

To evaluate the quantitativity of this method, we constructed the calibration curves for L-Glu and GABA, where the calibration ranges of L-Glu and GABA were 250–10000 and 2.5–100 ng mL^{-1}, respectively. Both calibration curves exhibited sufficient linearity ($R > 0.999$). Thus, we validated this method with the QC samples. As listed in Table 2, the intra- and inter-day accuracies and precisions were 0.4%–7.5% and 1.7%–5.4% for L-Glu, respectively, and 0.1%–4.8% and 2.1%–5.7% for GABA, respectively, demonstrating the high reproducibility of the method. The stability of the QC samples was also evaluated. As shown in Table S1, there was no change between each peak area ratio before and after 24h preservation at 4°C, demonstrating that the L-Glu and GABA were stable in aCSF for 24h at 4°C. To evaluate the specificity of the

Table 2
Validation results.

Compound name	Linearity (R)	Range (ng mL^{-1})	QC[a] (ng mL^{-1})	Intra-day (n = 6)		Inter-day (n = 6)	
				Precision RSD[b] (%)	Accuracy RE[c] (%)	Precision RSD (%)	Accuracy RE (%)
L-glutamic acid	0.999	250–10000	800	1.7%	−5.1%	2.2%	−7.5%
			4000	3.4%	−4.4%	5.1%	−3.6%
			8000	4.1%	−0.4%	5.4%	−5.0%
GABA	0.999	2.5–100	8.0	4.0%	−4.8%	4.3%	−3.5%
			40	4.7%	1.8%	5.7%	4.3%
			80	2.1%	−0.1%	3.6%	−2.7%

[a] QC: quality control.
[b] RSD: relative standard deviation.
[c] RE: mean relative error.

method, blank aCSF was measured. As shown in Fig. S2, L-Glu and GABA were not detected in blank aCSF. Also, we demonstrated chronograms of the lowest calibrant for L-Glu (250 ng mL^{-1}) and GABA (2.5 ng mL^{-1}) in Fig. S2 as the reference data. The lower limit of detection (LLOD) and the lower limit of quantification (LLOQ) were calculated according to our previous study [23]. LLOD and LLOQ were 94 and 286 ng mL^{-1} for L-Glu and 0.66 and 2.0 ng mL^{-1} for GABA, respectively (Table S4).

To evaluate the matrix effects between aCSF and high-K^+ aCSF, we prepared their spiked samples in which the concentrations of L-Glu and GABA were adjusted to 800 and 8.0 ng mL^{-1}, respectively. We analyzed the spiked aCSF and high-K^+ aCSF samples, and no matrix effect was observed between them (Fig. S3). Welch's *t*-test was performed for evaluating matrix effects by the R software [35].

3.3. 95% CI determined by Bayesian state-space model

In previous studies, statistical analyzes were performed for each time point data, which were obtained by averaging different individuals' values at each time point [8,27,28]. As mentioned above, this approach is somewhat inappropriate for evaluating time-series data, and Ngernsutivorakul et al. proposed a new approach using a general linear model [29]. Additionally, use of the Bayesian state-space model is acceptable for such time-series data, particularly for microdialysis data. In this study, thus, we adopted the Bayesian state-space model defined by Eq. (1) and determined the 95% CI. Based on the 95% CI, we detected abnormal changes in each mouse, which were caused by high-K^+-induced depolarization, as described later.

3.4. Extracellular L-Glu and GABA levels in microdialysates

To evaluate the feasibility of this methodology, extracellular L-Glu and GABA were collected from free-moving mice by in vivo microdialysis (n = 2). We monitored the local releases of L-Glu and GABA from the presynaptic terminal by high-K^+-induced depolarization [7,8,36]. The concentrations of L-Glu and GABA were stable at the basal levels for ca. 30 min (Fig. 3). Immediately after pre-aCSF was changed into high-K^+ aCSF at 30 min, the L-Glu level increased to ca. two-fold basal level within 10 min, although it reduced to a 0.5-fold basal level, which was maintained for ca. 50 min (50–100 min) (Figs. 3a–1 and 3b-1). After changing the perfusate to post-aCSF at 90 min, the L-Glu level slowly recovered to its basal level (90–120 min). When pre-aCSF was changed into high-K^+ aCSF at 30 min, the GABA levels did not immediately respond to this change, and their levels were kept at the basal level for 5 min (Figs. 3a–2 and 3b-2). However, the GABA levels slowly increased and achieved ca. seven-fold basal levels at the maximum. Moreover, these levels were maintained for an additional ca. 65 min (40–105 min). After perfusate was changed into post-aCSF, the GABA level decreased to the basal level, which was maintained for ca. 40 min (110–150 min).

These findings corresponded well with the results of previous reports (Table 3), and the concentration levels of L-Glu and GABA in the microdialysates were significantly increased by high-K^+ perfusion. In our study, we observed the concentration changes of L-Glu and GABA in the mouse striatum, where L-Glu was released from the corticostriatal afferents and GABA was released from the GABAergic interneurons [37,38]. In particular, Defaix et al. demonstrated that the concentration level of GABA in the microdialysate of the prefrontal cortex of a mouse attained the highest at ca. 15 min after the L-Glu level reached the

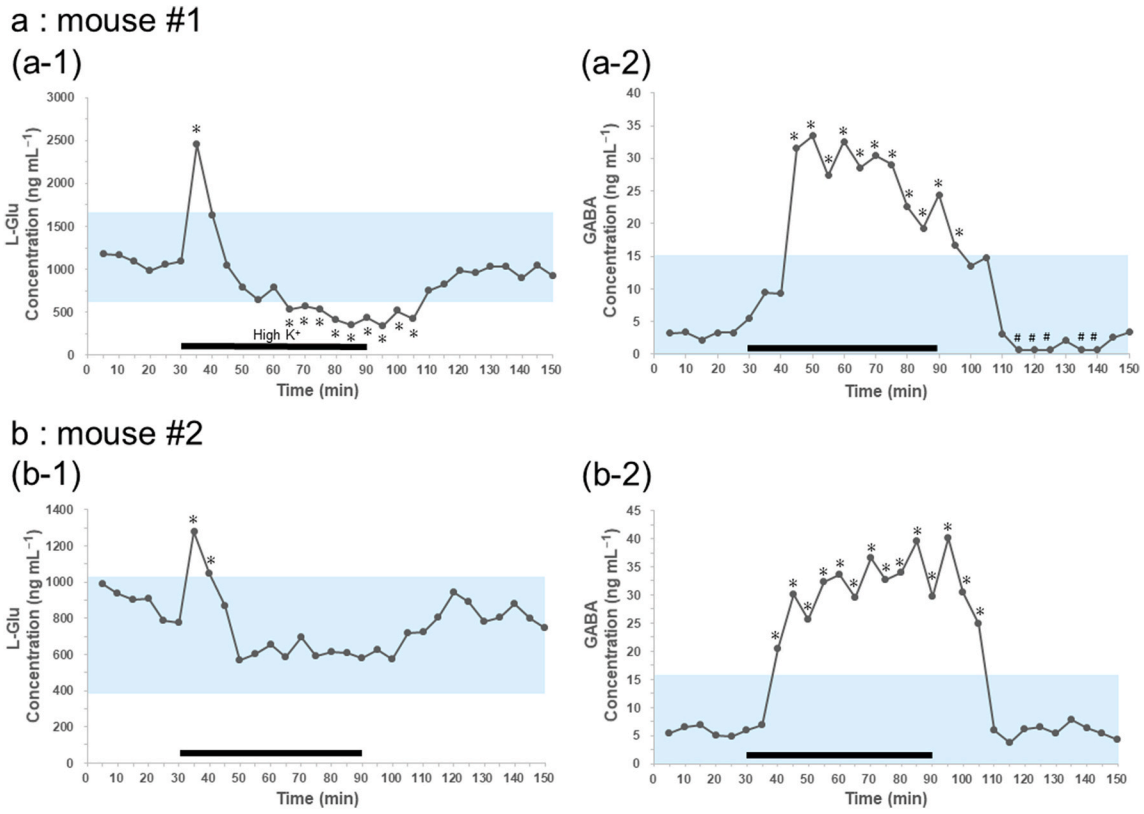

Fig. 3. Quantitative analyses of the extracellular L-Glu and GABA levels every 5 min in the mouse striatum (n = 2). Time-course changes in extracellular (a-1 and b-1) L-Glu and (a-2 and b-2) GABA levels in the microdialysate every 5 min. At 30 min, aCSF was replaced to high-K^+ aCSF, which was maintained for 60 min (black bar). 95% CI of the first ten-point data is shown in blue. Asterisk sign (*) indicate values that are outside the 95% CI. Hash sign (#) in (a-2) indicates values that are under LLOQ but over LLOD. These data are tentatively plotted by the value determined as (LLOQ−LLOD)/2. (For interpretation of the references to color in this figure legend, the reader is referred to the Web version of this article.)

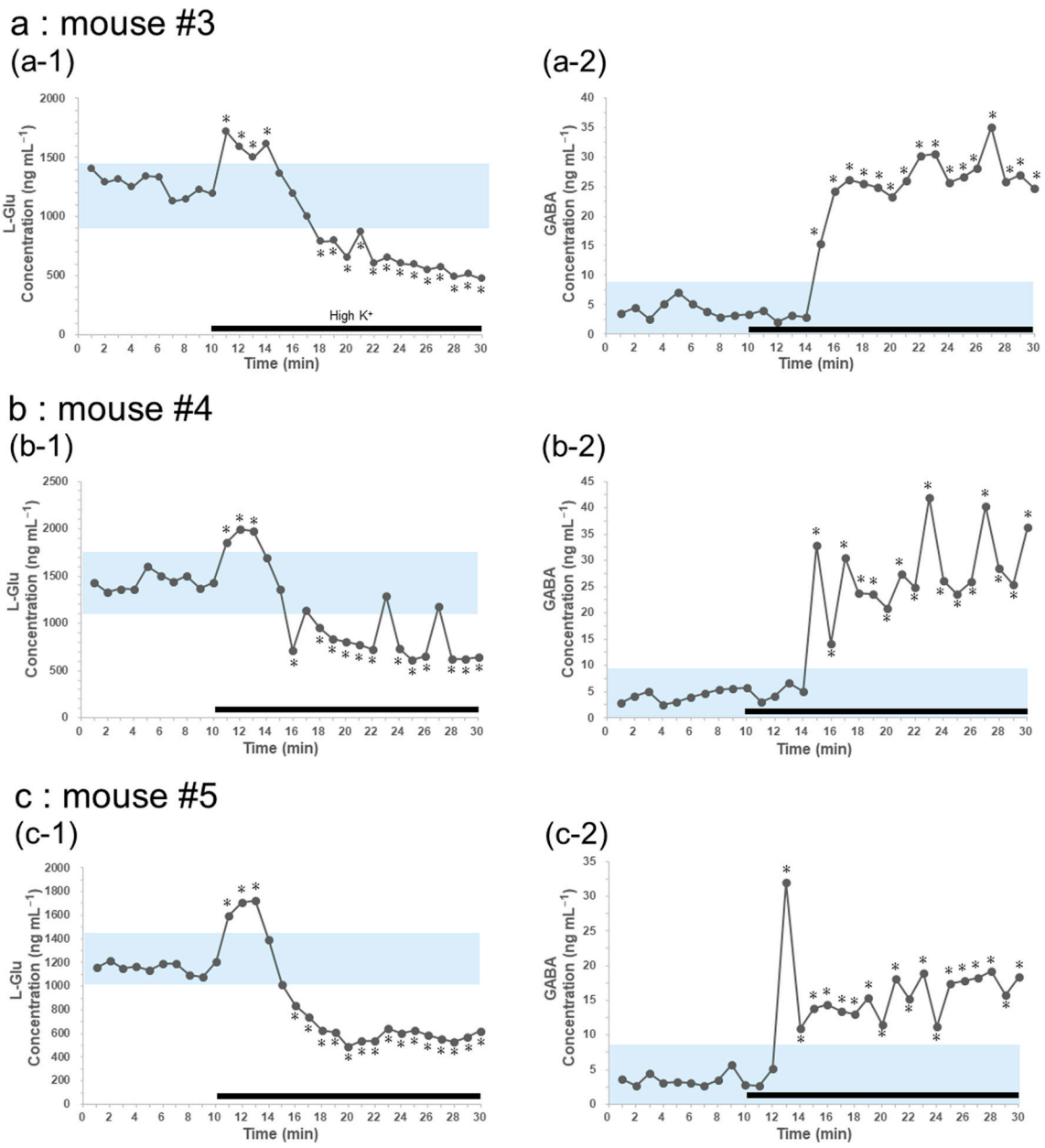

Fig. 4. Quantitative analyses of the L-Glu and GABA levels every 1 min in the mouse striatum (n = 3). Time-course changes in (a-1, b-1, and c-1) L-Glu and (a-2, b-2, and c-2) GABA levels in the microdialysate every 1 min. At 10 min, aCSF was replaced to high-K^+ aCSF, which was maintained for 20 min (black bar). The 95% CI of the first ten-point data is shown in blue. Asterisk indicate values that are outside the 95% CI. (For interpretation of the references to color in this figure legend, the reader is referred to the Web version of this article.)

Table 3
Comparison of the responses of L-Glu and GABA to high-K^+-induced depolarization in the previous studies and this study.

Brain regions	Animals	Maximum-fold changes		[K^+] (mM), Deporalization time (min)	Flow rates (μL min^{-1})	Ref.
		L-Glu	GABA			
mPFC	C57BL/6 mouse	3-fold	10-fold	120, 15	1.0	[8]
Globus pallidus	Wister rat	8-fold	14-fold	100, 20	2.0	[7]
Striatum	Sprague-Dawley rat	8-fold	18-fold	100, 1.0	0.1	[29]
Striatum	ICR mouse	2-fold	7-fold	100, 60	3.0	This study

mPFC: medial prefrontal cortex.

highest. As shown in Fig. 3a and b, the same phenomena were observed in our study. No individual difference was observed for GABA between the two mice (Figs. 3a–2 and 3b-2). However, the L-Glu level was below the basal level from 65 to 105 min in one of the mice (no. 1, Fig. 3a–1), though this phenomenon was not observed in the other mouse (no. 2, Fig. 3b–1). To further evaluate the phenomena in detail, additional experiments were performed using additional mice (n = 3). Here, the microdialysates were collected at a 1 min interval to observe the

aforementioned phenomena with a high temporal resolution, where the concentration levels of L-Glu and GABA were monitored for 20 min after high-K^+ perfusion. As shown in Figs. 4a–1, 4b-1, and 4c-1, the L-Glu level increased significantly in just 1 min after the high-K^+ perfusion of the three mice, and the level was maintained for 3 min. Afterward, the L-Glu level of each mouse decreased and was below each basal level, falling outside each 95% CI for 15 min, except for the time points of mouse no. 4 (7, 13, and 17 min) after the high-K^+ perfusion (Fig. 4b–1).

As described above, the L-Glu level of mouse no. 2 was within 95% CI from 65 to 105 min (Fig. 3b–1), although those of mice nos. 3, 4, and 5 were below 95% CI after the levels decreased. These results suggested that the measurement with a temporal resolution of 1 min was required to capture the subtle changes in the L-Glu levels by high-K^+-induced depolarization.

The decrease in the L-Glu level below the basal level could be caused by the uptake of extracellular glutamate via astrocytes [39–41]. In the striatum, astrocytes, which are mostly located around the glutamatergic synapse and glutamate transporter 1 (GLT-1) that is expressed by astrocytes, regulate the extracellular glutamate concentrations. GLT-1 is a Na^+-dependent transporter, which is co-localized with Na^+/K^+- ATPases in astrocytes [42,43]. When the extracellular K^+ concentration increased, Na^+ was complimentarily released from astrocytes by Na^+/K^+-ATPases, which facilitated GLT-1 and its uptake of extracellular L-Glu into astrocytes.

After the high-K^+ perfusion, GABA levels gradually increased in 5 min, after which they were maintained for 15 min (Figs. 4a–2, 4b-2, and 4c-2). GABA is released from the GABAergic interneurons when high-K^+ is perfused in the striatum. It is well-known that a Na^+/Cl^- dependent GABA transporter 3 (GAT-3) uptakes extracellular GABA to astrocytes and is upregulated by Cl^- [44,45]. However, the concentration of Cl^- is unchanged under this condition during the high-K^+ aCSF perfusion, whereas GAT-3 is not promoted by GABA uptake.

3.5. Comparison of the present method with previous ones

As shown in Table 4, Ngernsutivorakul et al. demonstrated that the concentrations of L-Glu and GABA are 8- and 18-fold higher compared with that of each basal level [29]. Their method achieved a temporal resolution of 6 s, which was the highest in previous studies (Table 4). In other studies on the simultaneous analyses of L-Glu and GABA in microdialysates, the temporal resolutions of their LC/MS/MS-based methods were generally 15–20 min [7,8] because they required a large sample volume. In contrast, the sample requirement of our PESI/MS/MS-based method was low (3 μL) and achieved a temporal resolution of 1 min. Moreover, our methods were validated using three QC samples, demonstrating that intra- and inter-day quantitativities of the methods were verified.

Additionally, the observation times were different in the previous studies. For example, Ngernsutivorakul et al. analyzed the L-Glu and GABA levels for 1.6 min by droplet-based microfluidics coupled with nanoelectrospray ionization mass spectrometry (nESI-MS). Buck et al. and Defaix et al. reported that the changes in the L-Glu and GABA levels were monitored for more than 120 min by LC/MS/MS-based methods [7,8], whereas our method could monitor the changes in the L-Glu and GABA levels in 30 and 150 min with 1- and 5-min temporal resolution, respectively. The observation time and temporal resolution were flexible because of the low sample volume requirement of our method (3 μL) and the non-requirement of tedious sample preparation. Furthermore, PESI/MS/MS enabled us to perform direct analyses of microdialysates and the data acquisition time was just 0.5 min per run, demonstrating its high operativity.

Although other targeted neurotransmitters, e.g., glutamine (Gln) and acetylcholine (Ach), were monitored in the previous studies by nESI-MS or LC/MS/MS, the PESI/MS/MS-based method could also analyze Gln and Ach for the following reasons: 1) PESI/MS/MS detected Gln even in intact mouse brain samples in our previous study [22,24,25]. Ngernsutivorakul et al. reported that the Gln levels in the microdialysate were 1000–1500 ng mL^{-1}, and those could be adequate for PESI/MS/MS. 2) In our preliminary experiment, 0.5 ng mL^{-1} Ach in aCSF could be measured by PESI/MS/MS (data not shown). Ngernsutivorakul et al. reported that the Ach levels in the microdialysate were 0.3–4.4 ng mL^{-1}, and these could be monitored by PESI/MS/MS. Furthermore, online microdialysis could be achieved by PESI/MS/MS, where the microdialysates would be continuously supplied to the PESI ion source. Our group has developed a special device that achieved a higher temporal resolution than that of this method, for online microdialysis employing PESI/MS/MS (patent pending).

Table 4
Comparison of the temporal resolutions of the analytical methods in previous studies and this study.

Analytes	Temporal resolutions (min)	Methods	Brain regions	Ref.
L-Glu, GABA, Gln, Ach	0.1	nESI-MS	Striatum	[29]
L-Glu, GABA	1	PESI/MS/MS	Striatum	This study
L-Glu, GABA, Gln	15	LC/MS/MS	mPFC	[8]
L-Glu, GABA	20	LC/MS/MS	Globus pallidus	[7]

nESI-MS: nanoelectrospray ionization (nESI) mass spectrometry, Gln: glutamine, Ach: acetylcholine.

4. Conclusion

In this study, we reported the combination of PESI/MS/MS with the microdialysis technique to monitor extracellular L-Glu and GABA levels in mouse striatum without tedious sample preparation. We optimized the MS parameters with the authentic standards and constructed the calibration curves, which exhibited sufficient linearity ($R > 0.999$). We validated this method using QC samples, which demonstrated that the intra- and inter-day accuracy and precision were 0.4%–7.5% and 1.7%–5.4% for L-Glu, respectively, and 0.1%–4.8% and 2.1%–5.7% for GABA, respectively. To evaluate the feasibility of this method, we applied it to high-K^+-induced depolarization and successfully monitored changes in the L-Glu and GABA levels in microdialysate by depolarization at 1 and 5 min intervals for 30 and 150 min, respectively. We also demonstrated that the Bayesian state-space model was highly effective in evaluating the time-series data obtained by microdialysis. As far as we know, this is the first report to show application of the Bayesian state-space model to microdialysis data. This methodology using PESI/MS/MS and the Bayesian state-space model allowed the easy monitoring of neurotransmitters at high temporal resolutions and appropriate data interpretation considering autocorrelation of time-series data, which will reveal the hidden pathological mechanisms of brain diseases like PD and HD in the future.

Credit author statement

Daisuke Kawakami: Conceptualization, Methodology, Validation, Formal analysis, Data curation, Investigation, Visualization, Resources, Writing - original draft, Writing - review & editing. **Mitsuki Tsuchiya:** Investigation, Resources. **Tasuku Murata:** Methodology, Resources. **Akira Iguchi:** Methodology, Formal analysis, Writing - review & editing. **Kei Zaitsu:** Conceptualization, Methodology, Software, Formal analysis, Data curation, Resources, Writing - original draft, Writing - review & editing, Project administration, Funding acquisition, Supervision.

Declaration of competing interest

The authors declare that they have no known competing financial interests or personal relationships that could have appeared to influence the work reported in this paper.

Acknowledgments

This work was supported by JSPS KAKENHI Grant Number 21H03793 and 20H05700. We are very grateful to Dr. Tastu Fuwa for instructing us how to perform his special microdialysis technique. We would like to thank an anonymous reviewer who strongly improved this manuscript with the feedback and comments.

Appendix A. Supplementary data

Supplementary data to this article can be found online at https://doi.org/10.1016/j.talanta.2021.122620.

References

[1] A.C. Kreitzer, R.C. Malenka, Striatal plasticity and basal ganglia circuit function, Neuron 60 (2008) 543–554, https://doi.org/10.1016/j.neuron.2008.11.005.
[2] R.L. Albin, A.B. Young, J.B. Penney, The functional anatomy of basal ganglia disorders, Trends Neurosci. 12 (1989) 366–375, https://doi.org/10.1016/0166-2236(89)90074-x.
[3] G.E. Alexander, M.D. Crutcher, Functional architecture of basal ganglia circuits: neural substrates of parallel processing, Trends Neurosci. 13 (1990) 266–271, https://doi.org/10.1016/0166-2236(90)90107-l.
[4] M.R. DeLong, Primate models of movement disorders of basal ganglia origin, Trends Neurosci. 13 (1990) 281–285, https://doi.org/10.1016/0166-2236(90)90110-v.
[5] F. Blandini, R.H. Porter, J.T. Greenamyre, Glutamate and Parkinson's disease, Mol. Neurobiol. 12 (1996) 73–94, https://doi.org/10.1007/BF02740748.
[6] C.A. Ross, E.H. Aylward, E.J. Wild, D.R. Langbehn, J.D. Long, J.H. Warner, R. I. Scahill, B.R. Leavitt, J.C. Stout, J.S. Paulsen, R. Reilmann, P.G. Unschuld, A. Wexler, R.L. Margolis, S.J. Tabrizi, Huntington disease: natural history, biomarkers and prospects for therapeutics, Nat. Rev. Neurol. 10 (2014) 204–216, https://doi.org/10.1038/nrneurol.2014.24.
[7] K. Buck, P. Voehringer, B. Ferger, Rapid analysis of GABA and glutamate in microdialysis samples using high performance liquid chromatography and tandem mass spectrometry, J. Neurosci. Methods 182 (2009) 78–84, https://doi.org/10.1016/j.jneumeth.2009.05.018.
[8] C. Defaix, A. Solgadi, T.H. Pham, A.M. Gardier, P. Chaminade, L. Tritschler, Rapid analysis of glutamate, glutamine and GABA in mice frontal cortex microdialysis samples using HPLC coupled to electrospray tandem mass spectrometry, J. Pharmaceut. Biomed. Anal. 152 (2018) 31–38, https://doi.org/10.1016/j.jpba.2018.01.039.
[9] A.G. Zestos, H. Luna-Munguia, W.C. Stacey, R.T. Kennedy, Use and future prospects of in vivo microdialysis for epilepsy studies, ACS Chem. Neurosci. 10 (2019) 1875–1883, https://doi.org/10.1021/acschemneuro.8b00271.
[10] A.G. Zestos, R.T. Kennedy, Microdialysis coupled with LC-MS/MS for in vivo neurochemical monitoring, AAPS J. 19 (2017) 1284–1293, https://doi.org/10.1208/s12248-017-0114-4.
[11] M. Okada, K. Fukuyama, T. Nakano, Y. Ueda, Pharmacological discrimination of effects of MK801 on thalamocortical, mesothalamic, and mesocortical transmissions, Biomolecules 9 (2019), https://doi.org/10.3390/biom9110746.
[12] S. Schmidt, S. Martinsson, In vivo/in vitro microdialysis coupled to capillary LC-LIF, Biomed, Chromatography 12 (1998) 109–110, https://doi.org/10.1002/(SICI)1099-0801(199805/06)12:3<109::AID-BMC770>3.0.CO;2-V.
[13] K.T. Ngo, E.L. Varner, A.C. Michael, S.G. Weber, Monitoring dopamine responses to potassium ion and nomifensine by in vivo microdialysis with online liquid chromatography at one-minute resolution, ACS Chem. Neurosci. 8 (2017) 329–338, https://doi.org/10.1021/acschemneuro.6b00383.
[14] S. Xu, C. Li, H. Zhou, L. Yu, L. Deng, J. Zhu, H. Wan, Y. He, A study on acetylglutamine pharmacokinetics in rat blood and brain based on liquid chromatography-tandem mass spectrometry and microdialysis technique, Front. Pharmacol. 11 (2020) 508, https://doi.org/10.3389/fphar.2020.00508.
[15] S. Xie, J. Aspromonte, A. Balla, H. Sershen, D.C. Javitt, T.B. Cooper, Sensitive and simple gas chromatographic-mass spectrometric determination for amphetamine in microdialysate and ultrafiltrate samples, J Chromatogr B Analyt Technol Biomed Life Sci 805 (2004) 27–31, https://doi.org/10.1016/j.jchromb.2004.02.001.
[16] A. Santos-Fandila, A. Zafra-Gomez, A. Barranco, A. Navalon, R. Rueda, M. Ramirez, Quantitative determination of neurotransmitters, metabolites and derivates in microdialysates by UHPLC-tandem mass spectrometry, Talanta 114 (2013) 79–89, https://doi.org/10.1016/j.talanta.2013.03.082.
[17] M.S. Bergh, I.L. Bogen, E. Lundanes, A.M.L. Oiestad, Validated methods for determination of neurotransmitters and metabolites in rodent brain tissue and extracellular fluid by reversed phase UHPLC-MS/MS, J. Chromatogr. B Analyt. Technol. Biomed. Life Sci. 1028 (2016) 120–129, https://doi.org/10.1016/j.jchromb.2016.06.011.
[18] Y.C. Huang, H.H. Chung, E. Dutkiewicz, C.L. Chen, H.Y. Hsieh, B.R. Chen, M. Y. Wang, C.C. Hsu, Predicting breast cancer by paper spray ion mobility spectrometry mass spectrometry and machine learning, Anal. Chem. (2019), https://doi.org/10.1021/acs.analchem.9b03966.
[19] D. Lostun, C.J. Perez, P. Licence, D.A. Barrett, D.R. Ifa, Reactive DESI-MS imaging of biological tissues with dicationic ion-pairing compounds, Anal. Chem. 87 (2015) 3286–3293, https://doi.org/10.1021/ac5042445.
[20] X. Gong, Y. Zhao, S. Cai, S. Fu, C. Yang, S. Zhang, X. Zhang, Single cell analysis with probe ESI-mass spectrometry: detection of metabolites at cellular and subcellular levels, Anal. Chem. 86 (2014) 3809–3816, https://doi.org/10.1021/ac500882e.
[21] J. Laskin, I. Lanekoff, Ambient mass spectrometry imaging using direct liquid extraction techniques, Anal. Chem. 88 (2016) 52–73, https://doi.org/10.1021/acs.analchem.5b04188.
[22] Y. Hayashi, K. Zaitsu, T. Murata, T. Ohara, S. Moreau, M. Kusano, H. Tanihata, H. Tsuchihashi, A. Ishii, T. Ishikawa, Intact metabolite profiling of mouse brain by probe electrospray ionization/triple quadrupole tandem mass spectrometry (PESI/MS/MS) and its potential use for local distribution analysis of the brain, Anal. Chim. Acta 983 (2017) 160–165, https://doi.org/10.1016/j.aca.2017.06.047.
[23] K. Hisatsune, T. Murata, K. Ogata, M. Hida, A. Ishii, H. Tsuchihashi, Y. Hayashi, K. Zaitsu, RECiQ: a rapid and easy method for determining cyanide intoxication by cyanide and 2-Aminothiazoline-4-carboxylic acid quantification in the human blood using probe electrospray ionization tandem mass spectrometry, ACS Omega 5 (2020) 23351–23357, https://doi.org/10.1021/acsomega.0c03229.
[24] K. Zaitsu, S. Eguchi, T. Ohara, K. Kondo, A. Ishii, H. Tsuchihashi, T. Kawamata, A. Iguchi, PiTMaP: a new analytical platform for high-throughput direct metabolome analysis by probe electrospray ionization/tandem mass spectrometry using an R software-based data pipeline, Anal. Chem. 92 (2020) 8514–8522, https://doi.org/10.1021/acs.analchem.0c01271.
[25] K. Zaitsu, Y. Hayashi, T. Murata, T. Ohara, K. Nakagiri, M. Kusano, H. Nakajima, T. Nakajima, T. Ishikawa, H. Tsuchihashi, A. Ishii, Intact endogenous metabolite analysis of mice liver by probe electrospray ionization/triple quadrupole tandem mass spectrometry and its preliminary application to in vivo real-time analysis, Anal. Chem. 88 (2016) 3556–3561, https://doi.org/10.1021/acs.analchem.5b04046.
[26] K. Zaitsu, Y. Hayashi, T. Murata, K. Yokota, T. Ohara, M. Kusano, H. Tsuchihashi, T. Ishikawa, A. Ishii, K. Ogata, H. Tanihata, In vivo real-time monitoring system using probe electrospray ionization/tandem mass spectrometry for metabolites in mouse brain, Anal. Chem. 90 (2018) 4695–4701, https://doi.org/10.1021/acs.analchem.7b05291.
[27] A. Giuffrida, L.H. Parsons, T.M. Kerr, F. Rodriguez de Fonseca, M. Navarro, D. Piomelli, Dopamine activation of endogenous cannabinoid signaling in dorsal striatum, Nat. Neurosci. 2 (1999) 358–363, https://doi.org/10.1038/7268.
[28] P. Tuma, B. Sommerova, M. Siklova, Monitoring of adipose tissue metabolism using microdialysis and capillary electrophoresis with contactless conductivity detection, Talanta 192 (2019) 380–386, https://doi.org/10.1016/j.talanta.2018.09.076.
[29] T. Ngernsutivorakul, D.J. Steyer, A.C. Valenta, R.T. Kennedy, In vivo chemical monitoring at high spatiotemporal resolution using microfabricated sampling probes and droplet-based microfluidics coupled to mass spectrometry, Anal. Chem. 90 (2018) 10943–10950, https://doi.org/10.1021/acs.analchem.8b02468.
[30] T. Fuwa, J. Suzuki, T. Tanaka, A. Inomata, Y. Honda, T. Kodama, Novel psychoactive benzofurans strongly increase extracellular serotonin level in mouse corpus striatum, J. Toxicol. Sci. 41 (2016) 329–337, https://doi.org/10.2131/jts.41.329.
[31] B. Carpenter, A. Gelman, M.D. Hoffman, D. Lee, B. Goodrich, M. Betancourt, M. Brubaker, J. Guo, P. Li, A. Riddell, Stan : a probabilistic programming language, J. Stat. Software 76 (2017), https://doi.org/10.18637/jss.v076.i01.
[32] K. Brodersen, F. G, J. K, N. R, S.L. S, Inferring causal impact using Bayesian structural time-series models, Ann. Appl. Stat. 9 (2015) 247–274, https://doi.org/10.1214/14-AOAS788.
[33] S. Särkkä, Bayesian Filtering and Smoothing, third ed., Cambridge University Press, 2014.
[34] K. Hiraoka, K. Nishidate, K. Mori, D. Asakawa, S. Suzuki, Development of probe electrospray using a solid needle, Rapid Commun. Mass Spectrom. 21 (2007) 3139–3144, https://doi.org/10.1002/rcm.3201.
[35] R. Ihaka, R. Gentleman, A language for data analysis and graphics, J. Comput. Graph Stat. 5 (1996) 299–314.
[36] W. Timmerman, B.H. Westerink, Brain microdialysis of GABA and glutamate: what does it signify? Synapse 27 (1997) 242–261, https://doi.org/10.1002/(SICI)1098-2396(199711)27:3<242::AID-SYN9>3.0.CO;2-D.
[37] A.E. Girasole, A.B. Nelson, Probing striatal microcircuitry to understand the functional role of cholinergic interneurons, Mov. Disord. 30 (2015) 1306–1318, https://doi.org/10.1002/mds.26340.
[38] Y. Kubota, Y. Kawaguchi, Dependence of GABAergic synaptic areas on the interneuron type and target size, J. Neurosci. 20 (2000) 375–386.
[39] D.A. Baker, Z.X. Xi, H. Shen, C.J. Swanson, P.W. Kalivas, The origin and neuronal function of in vivo nonsynaptic glutamate, J. Neurosci. 22 (2002) 9134–9141.
[40] M. Fouyssac, D. Belin, Beyond drug-induced alteration of glutamate homeostasis, astrocytes may contribute to dopamine-dependent intrastriatal functional shifts that underlie the development of drug addiction: a working hypothesis, Eur. J. Neurosci. 50 (2019) 3014–3027, https://doi.org/10.1111/ejn.14416.
[41] C. Perego, C. Vanoni, M. Bossi, S. Massari, H. Basudev, R. Longhi, G. Pietrini, The GLT-1 and GLAST glutamate transporters are expressed on morphologically

distinct astrocytes and regulated by neuronal activity in primary hippocampal cocultures, J. Neurochem. 75 (2000) 1076–1084, https://doi.org/10.1046/j.1471-4159.2000.0751076.x.
[42] C.M. Anderson, R.A. Swanson, Astrocyte glutamate transport: review of properties, regulation, and physiological functions, Glia 32 (2000) 1–14.
[43] N. Cholet, L. Pellerin, P.J. Magistretti, E. Hamel, Similar perisynaptic glial localization for the Na+,K+-ATPase alpha 2 subunit and the glutamate transporters GLAST and GLT-1 in the rat somatosensory cortex, Cerebr. Cortex 12 (2002) 515–525, https://doi.org/10.1093/cercor/12.5.515.
[44] N.O. Dalby, Inhibition of gamma-aminobutyric acid uptake: anatomy, physiology and effects against epileptic seizures, Eur. J. Pharmacol. 479 (2003) 127–137, https://doi.org/10.1016/j.ejphar.2003.08.063.
[45] X.T. Jin, A. Galvan, T. Wichmann, Y. Smith, Localization and function of GABA transporters GAT-1 and GAT-3 in the basal ganglia, Front. Syst. Neurosci. 5 (2011) 63, https://doi.org/10.3389/fnsys.2011.00063.